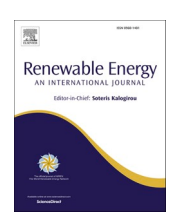
ELSEVIER

Contents lists available at ScienceDirect

# Renewable Energy

journal homepage: www.elsevier.com/locate/renene



# Cogeneration processes based on giant reed gasification combined with ORC and district heating for heat recovery: Comparative energy and exergy analysis

Mauro Prestipino <sup>a,\*</sup>, Antonio Piccolo <sup>a</sup>, Carlos Mourao Vilela <sup>b</sup>, Antonio Galvagno <sup>a,\*\*</sup>

#### ARTICLE INFO

Keywords:
Arundo donax
Exergy analysis
ORC
Combined heat and power
Energy crop
Thermodynamic sustainability

#### ABSTRACT

This research work develops a comprehensive exergy and energy assessment of a cogeneration process using Giant Reed as feedstock, which consists of a biomass dryer, a fluidized bed gasifier, an internal combustion engine operating in a cogeneration mode (CHP), and two different users for the cogenerated heat. One process layout uses cogenerated heat in a district heating network (CHP + DH layout). In the second process layout, the cogenerated heat produces additional electricity through an Organic Rankine Cycle (CHP + ORC layout). In addition to the performance of reed gasification (cold gas efficiency about 0.6), the results showed that the highest rational efficiency was reached in the cogeneration unit, while the highest relative irreversibilities were found in the gasifier and the dryer. The overall energy efficiencies are 0.46 and 0.22 for the CHP + DH and CHP + ORC layouts, respectively, while the overall exergy efficiencies are 0.21 and 0.20. The difference in the sustainability index is just 2 %. The results and methods of this research work can be used to properly design Giant Reed (or similar biomass) gasification plants and bioenergy systems for combined heat and power production, and developing case-studies considering the sustainable use of this feedstock according to a thermodynamic approach based on the second principle.

#### 1. Introduction

On a global scale, there is a growing interest in exploring renewable and sustainable energy sources to meet the increasing energy demand. Renewable sources are gaining attention due to their abundance and potential low environmental impact [1]. In recent years, electrification has been one of the most promising pathways for decarbonizing different economic sectors [2,3]. This will include, but is not limited to, transportation [3] and domestic heating [4]. When direct electrification is not feasible or convenient, industrial heating will move to indirect electrification through the massive deployment of renewable hydrogen [5] and other alternative fuels [6]. The above pathways for energy transition involve the increase of electricity demand globally, which is also driven by the economic growth of developing countries [7]. Under this global energy context and perspective, renewable and sustainable primary energy sources are paramount. However, most renewable energy resources, such as wind and sun radiation, are not continuous,

while a stable source of clean energy is needed to stabilize the energy grids [8]. Among the variety of options to reach this goal, biomass and bioenergy have gained significant interest. Unlike fossil fuels that take a long time to regenerate, biomass can be replenished relatively quickly. When it burns, it releases carbon dioxide into the atmosphere, but this biogenic CO<sub>2</sub> is not considered a contributor to global warming [9]. Consequently, biomass power production can be regarded as carbon neutral if the supply chain is managed sustainably [10]. Biomass can be converted into different products (solid, liquid, or gas fuels and chemicals) using various technologies depending on the chemical and physical characteristics of the feedstock and the desired main product [11]. Among the different technologies, thermochemical gasification allows the conversion of biomass into bio-syngas that can feed an internal combustion engine, a gas turbine, or a fuel cell to produce power [12]. From the micro (0.05–0.2  $MW_e$ ) to the small-medium scale (0.2–2 MW<sub>e</sub>), internal combustion engines are very often used for combined heat and power production (CHP), also known as cogeneration. CHP

E-mail addresses: mprestipino@unime.it (M. Prestipino), agalvagno@unime.it (A. Galvagno).

<sup>&</sup>lt;sup>a</sup> University of Messina, Department of Engineering, Messina, Italy

<sup>&</sup>lt;sup>b</sup> TNO, Petten, the Netherlands

<sup>\*</sup> Corresponding author.

<sup>\*\*</sup> Corresponding author.

units based on internal combustion engines can recover heat from the intercooler, the lube oil, the engine's jacket water, and the exhaust gas. In the case of biomass gasification combined with a CHP unit, a certain fraction of the cogenerated heat is expected to be used for drying the feedstock, especially in the case of residual biomass [13]. Only a small fraction of the cogenerated heat is used for drying when the feedstock is a semi-dry biomass with low moisture content (20-30 % weight). This energy stream should be exploited and delivered to a user to maximize the sustainability of the whole process. If the gasification-CHP plant is not installed within a specific factory or integrated with a particular production process, two leading solutions exist for exploiting cogenerated heat. A system integration solution consists in district heating [14], whose feasibility is influenced by the location's climatic conditions. Another option is converting the cogenerated heat to electricity using an Organic Rankine Cycle (ORC) unit [15], which can be installed in any location covered by the electrical grid. The drawback of this process integration is that it has very low thermal-electrical efficiency, ranging from 7 % to 12 % [15]. In several case studies, these two integration solutions for the exploitation of cogenerated heat compete with each other, and the selection of one of the two should be based not only on economic analysis but also on the sustainability of resource utilization. Over the years, the concept of sustainability and resource depletion has been extended to thermodynamic analysis [16]. Thermodynamic analysis of energy systems based on exergy data can be used as a selection tool when different process configurations are compared and for process optimization [17].

Sigurjonsson and Clausen [18] introduced an innovative biomass-based SOFC polygeneration system to address the issues arising from intermittent energy sources like wind and solar energy. Through a comprehensive techno-economic analysis, they highlighted the significance of the district heating product for ensuring the economic viability of the polygeneration plant. They did not explore the ORC technology as an alternative to district heating.

François et al. [19] developed the energetic and exergetic analysis of a biomass gasification CHP plant, where the effects of biomass and bio-syngas pretreatment on the system's performance were assessed. As feedstock, it was used wood. The cogenerated heat was partially used for drying the feedstock, while the residual heat was used for district heating. The highest exergy efficiency was 30 % when feedstock was first dried naturally and then subjected to forced thermal drying using cogenerated heat [19]. However, the thermal loss of the hypothetical hot water distribution network was not taken into account. They identified as the best process configuration, from the exergy efficiency point of view, the case in which additional electricity production through steam turbines is applied instead of district heating. Nevertheless, heat-to-electricity conversion through steam turbines is not always an option when the temperature of the heat source is relatively low, as in the case of many CHP systems based on internal combustion engines or in the case of small to medium-scale gasifiers where the bio-syngas flow rates and temperature are not enough to justify the capital costs of the integration with the steam power plant. Wu et al. [20] conducted an exergy, exergoeconomic, and environmental analysis of a polygeneration system based on biomass gasification. They underlined the role of district heating in improving the exergy and environmental performance of the system when low-temperature heat recovery is applied. Nguyen and Gustavsson's [6] results confirmed that cost-effective solutions for more extensive district heating systems involve co-generating heat and electricity. In their study, Kabalina et al. [21] showed the benefits of retrofitting an existing district heating system by implementing a gasification unit for polygeneration. They carried out an exergy analysis of the whole system for different scenarios but did not include a detailed analysis of each stream and unit.

Yang et al. [22] developed a parametric optimization of a dual-loop ORC system fed by waste heat from a gas engine. They optimized the heat exchange area and the energy efficiency of the whole power production system, reaching the energy efficiency of the ORC unit in the

range of 8-10 %. Similarly, in the paper by Badescu et al. [23], the authors dealt with waste heat recovery from internal combustion engines at partial loads using an ORC cycle. In these studies [22,23], the exergy analysis of the proposed processes was not taken into account. Nevertheless, many other studies indicated the first and second principle analysis of ORC systems fed by waste heat from power production units based on biomass or waste gasification [24,25]. Most papers in which gasification is the biomass conversion unit, do not have internal combustion engines as the main power unit and do not consider the use and conversion of cogenerated heat. Another aspect that has not been exhaustively explored in literature is the possibility of consistently comparing the ORC solution with other heat recovery options, such as district heating. Furthermore, detailed thermodynamic analysis for each stream and unit, aiming to provide fundamental data for the improvement potentials and process replications and for building new case studies of bioenergy systems, is lacking in the current literature. Regarding the gasification of Arundo Donax, Manic et al. [26] carried out a recent theoretical study on pyrolysis and gasification of this feedstock. However, they did not present the syngas yield, a precise composition, or an experimental validation of the simulations. The process integration with a cogeneration unit is also missing. A relevant number of research works are available in the literature regarding Arundo Donax pyrolysis and, in some cases, pyrolysis combined with gasification [27]. Hence, experimental data on direct gasification of this feedstock in a continuous fluidized bed is missing in the literature. Consequently, there is a lack of available data for developing detailed case studies on bioenergy systems based on Arundo Donax gasification.

Indeed, in addition to the lack of comprehensive thermodynamic comparison and analysis of the ORC and district heating solutions integrated with gasification and internal combustion CHP, to the best of the authors' knowledge, the existing literature lacks in the investigation of Giant Reed (Arundo Donax) gasification coupled with a cogeneration power plant, which also excludes the exergy analysis of such systems. This limits the knowledge of the potential of such feedstock in gasification-based cogenerative systems.

This paper addresses the aforementioned literature gaps by examining the integration of Arundo Donax gasification with a combined heat and power (CHP) unit based on internal combustion technology. Two distinct cogenerated heat recovery solutions are explored, each represented by a different process layout: one focused on heat integration with a district heating network and the other utilizing a dual ORC for converting heat into electricity. A rigorous comparative analysis of these two process layouts is conducted using both first (energy) and second (exergy) law approaches, leveraging data obtained from AVEVA PRO/II simulations and original experimental studies on Arundo Donax gasification. The detailed exergy analysis covers all process streams and components, identifying inefficiencies and irreversibilities. This level of analysis enhances replicability for future research and enables targeted improvements in system design and operation.

From the above, the motivation for this research is to fill the following lack of literature works: i) exploring and unlocking the potential of Arundo Donax (Giant Reed) in cogeneration systems based on gasification of this feedstock in fluidized bed reactors; ii) comparing two different layouts differing in the heat use of net cogenerated heat starting from the same upstream conditions; iii) carrying out a comparative and detailed thermodynamic analysis based on energy and exergy data for the two investigated layouts aiming at assessing and uncovering the thermodynamic sustainability of the two different process integrations, while facilitating informed process selection, design, and the development of future case studies of bioenergy systems base on Arundo Donax gasification.

#### 2. Methods

#### 2.1. Process overview

The cogenerative bioenergy system under investigation is based on the experimental tests of giant reed gasification (Arundo Donax) and the simulations of the upstream and downstream processes integrated with this unit. The overview of the process integration is described in Fig. 1. The feedstock entering the system is semi-dry giant reed (Around Donax), directed to the drying unit where its water content is reduced from 20 % to 10 % (in mass). In the gasifier, the feedstock is converted to hot syngas (see the following sections for details on the feedstock and the operating conditions of the gasifier), which is then cooled for sensible heat recovery at the minimum temperature of 200 °C. This temperature limitation is set to avoid massive tar condensation. Then, the syngas at 200 °C passes through a scrubbing unit for tar abatment. Here the syngas is cooled to 30  $^{\circ}$ C, which is a temperature compatible with the internal combustion engine of the CHP unit. In this unit the cold syngas runs an internal combustion engine operating in cogeneration mode for the combined production of electricity and heat. A fraction of the cogenerated heat is directed to the drying unit. Two different scenarios differentiate the process layout depending on the technology used to exploit the net heat cogenerated in the CHP unit and the heat recovery section (by cooling the hot syngas). In one process layout (CHP + ORC layout), the cogenerated heat is converted into electricity by an Organic Rankine Cycle, while in the other process layout (CHP + DH layout), the cogenerated heat is used as low-temperature heat in a district heating network.

The process layouts, excluding the gasification unit, were simulated with the *AVEVA PRO/II Simulation* software (2022 version) at steady state conditions. The thermodynamic method used is the SRK. The input stream in the model is the syngas as it exits the reactor at 650  $^{\circ}$ C, whose flow rate and composition used in this work are obtained experimentally. The syngas flow rate is then scaled in the simulation model for a biomass flow rate of 1 t/h (on a dry basis). Specific syngas yield and compositions depend on the tested operating conditions, which are shown and selected in section 3.

The following sections describe the feedstock characterization and drying (section 2.2), the experimental gasification tests (section 2.3), the CHP unit (section 2.4), the two process layouts in detail (section 2.5), the calculations of process analysis (section 2.6).

#### 2.2. Giant reed characterization and drying

As mentioned above, in the presented bioenergy system Giant Reed (Arundo Donax) is assumed with 20 % (mass) of water content as it is delivered to the plant site. The ultimate and proximate analysis, on a dry basis, are reported in Table 1:

In the drying unit, the semi-dry feedstock is dried to reach 10~% water content before entering the gasification reactor (stream 1~ in Figs. 2~and 3) from the initial 20~% of the received feedstock. The energy demand of the drying unit is calculated according to the following equation:

$$\dot{Q}_{dryer} = \dot{m}_{biom} \frac{(1 - x_1) \bullet c_{p,biom} \bullet \Delta T + x_2 \Delta h_{ev} + x_1 \bullet c_{p,w} \bullet \Delta T)}{\eta_{th,dryer}}$$
(1)

Where  $x_I$  and  $x_2$  are the water mass fraction of feedstock at the entrance of the dryer and the mass fraction of water that evaporates, respectively.  $\Delta T$  is the considered temperature interval (80 °C),  $\Delta h_{ev}$  is the evaporation enthalpy of water at 100 °C, and  $c_{p,biom}$  (1.5 kJ/kgK) [28] and  $c_{p,w}$  (4.2 kJ/kgK) are the specific heat of dry biomass and water (considering them constant as the average value between 20 °C and 100 °C), respectively. The theoretical enengy demand of the dryer is divided by its thermal efficiency  $(\eta_{th,dryer})$ , which is set to 0.84 [29].

The energy input of the drying unit is the exhaust gas from the cogeneration unit, which is cooled down to the temperature range of  $150-200\,^{\circ}\text{C}$ . In the simulation model, the drying unit is modeled by a heat exchanger where the flue gas is cooled according to the heat duty calculated in Equation (1), which is the input data of the block.

**Table 1**Giant reed ultimate and proximate analysis.

| Ultimate analysis, dry basis [%wt] |               |                |                |               |                                   |  |  |  |
|------------------------------------|---------------|----------------|----------------|---------------|-----------------------------------|--|--|--|
| C                                  | C H N S O     |                |                |               |                                   |  |  |  |
| 46.30<br>%                         | 5.80 %        | 0.60 %         | 0.19 %         | 42.10 %       |                                   |  |  |  |
| Dro                                | After drying  |                |                |               |                                   |  |  |  |
|                                    | oximate analy | sis, dry basis | [70WL]         | As received   | Arter drying                      |  |  |  |
| Ash                                | Volatiles     | HHV<br>[MJ/kg] | LHV<br>[MJ/kg] | Water content | Water content [% <sub>w/w</sub> ] |  |  |  |

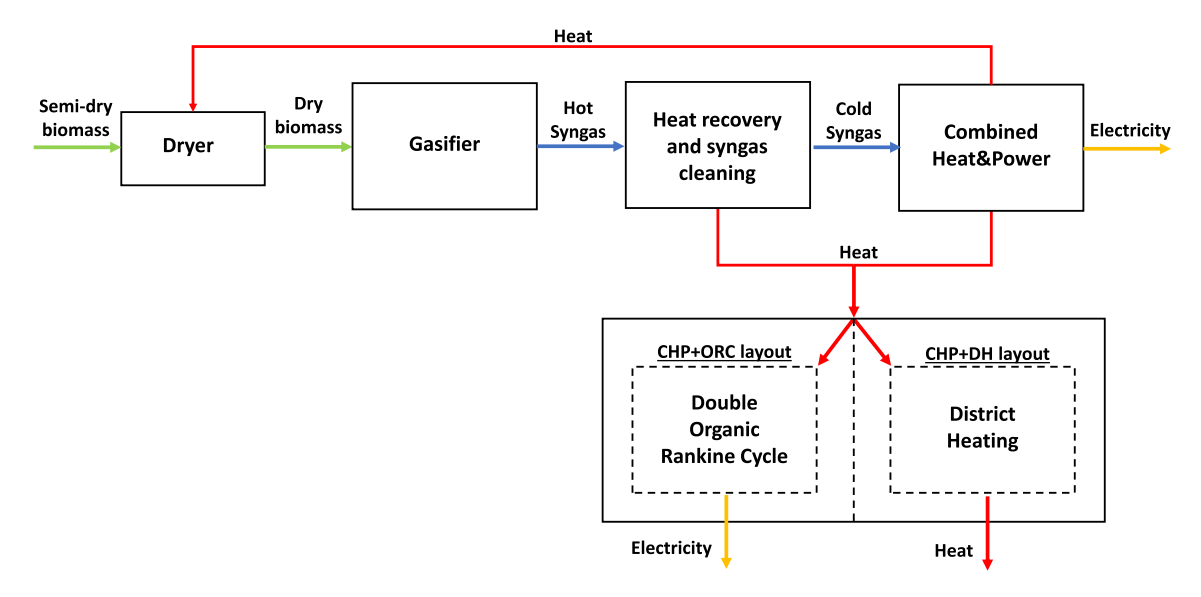


Fig. 1. Overview of the bioenergy process considering two process layouts.

**Table 2**Main operational features of the CHP unit.

| Parameter   | Value     | Units        |
|---|-----------|--------------|
| Low-temperature thermal efficiency, excluding flue gas $(\eta_{th\text{-}CHP})$ | 0.196     | [-]          |
| Flue gas temperature  | 464       | °C           |
| Flue gas yield (per unit of syngas flow)  | 3.09      | [kg/<br>Nm³] |
| Return/supply temperature low-T CHP heat recovery                               | 70/<br>80 | [°C]         |
| Electrcial efficiency (η <sub>el</sub> , <sub>CHP</sub> )                       | 0.368     | [-]          |
| Syngas temperature at reactor's exit  | 650       | [°C]         |

### 2.3. Gasification and syngas cooling

Experimental activities on the gasification of Giant Reed were performed in a lab-scale bubbling fluidized bed (BFB) reactor in the TNO laboratories in Petten (Netherlands). In this work, the reactor temperature of 850  $^{\circ}\text{C}$  and the air (as gasification medium) equivalence ratio of 0.3 are fixed process parameters for this study. The steam-to-biomass ratio (S/B) varies from 0 to 0.75 to assess the effects of steam on the gasification performance.

During the gasification tests, after passing through a hot filter, a condenser, and a HEPA filter, the producer gas is sent to a Varian  $\mu$ -GC CP4900 gas chromatograph to determine permanent gases sampled at 4-min intervals. This device is equipped with four gas channels and a

thermal conductivity detector (TCD). The bio-syngas flow rate is not directly measured. Instead, it is calculated from the mass balance of Neon, which is used as a tracer gas. A more detailed description of the gasification facility at TNO is described in previous works [30]. The performances of the gasifier were assessed by calculating the bio-syngas lower heating value (LHV), the bio-syngas yield ( $Y_{syn}$ ), and the cold gas efficiency (CGE), as reported below.

$$Y_{syn} = \frac{\dot{V}_{syn}}{\dot{m}_{biom}} \tag{2}$$

$$CGE = \frac{\dot{V}_{syn}LHV_{syn}}{\dot{m}_{biom}LHV_{biom}} \tag{3}$$

Where  $\dot{V}_{syn}$  and  $\dot{m}_{biom}$  are the volumetric flow rate of bio-syngas at normal conditions and the biomass flow rate. In particular, the biosyngas yield is reported per kilogram of biomass on a dry basis. The CGE is used as the reference performance indicator to select the best-performing S/B ratio. Once the operating condition is selected, the corresponding syngas composition and yield are used to create the input stream of the simulation model, which is the syngas at the reactor exit.

The study of the bio-syngas cleaning section is not the object of this study, so the detailed analysis of the scrubbing unit is not carried out. Indeed, several research works demonstrate how the tar content can be drastically reduced within an oil scrubbing unit [31]. The scrubbing unit is represented in the process layouts presented in this work because the

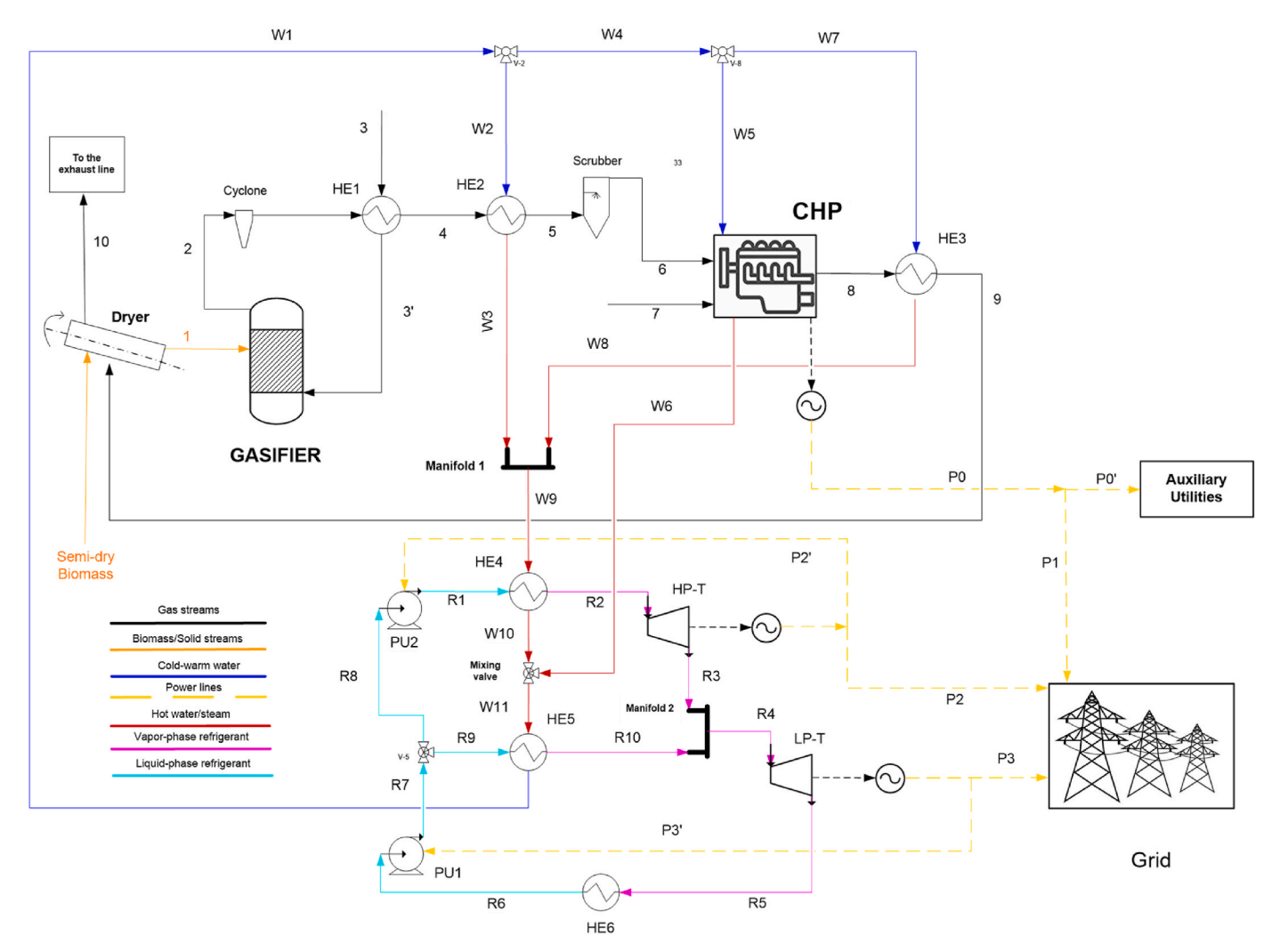


Fig. 2. CHP + ORC layout.

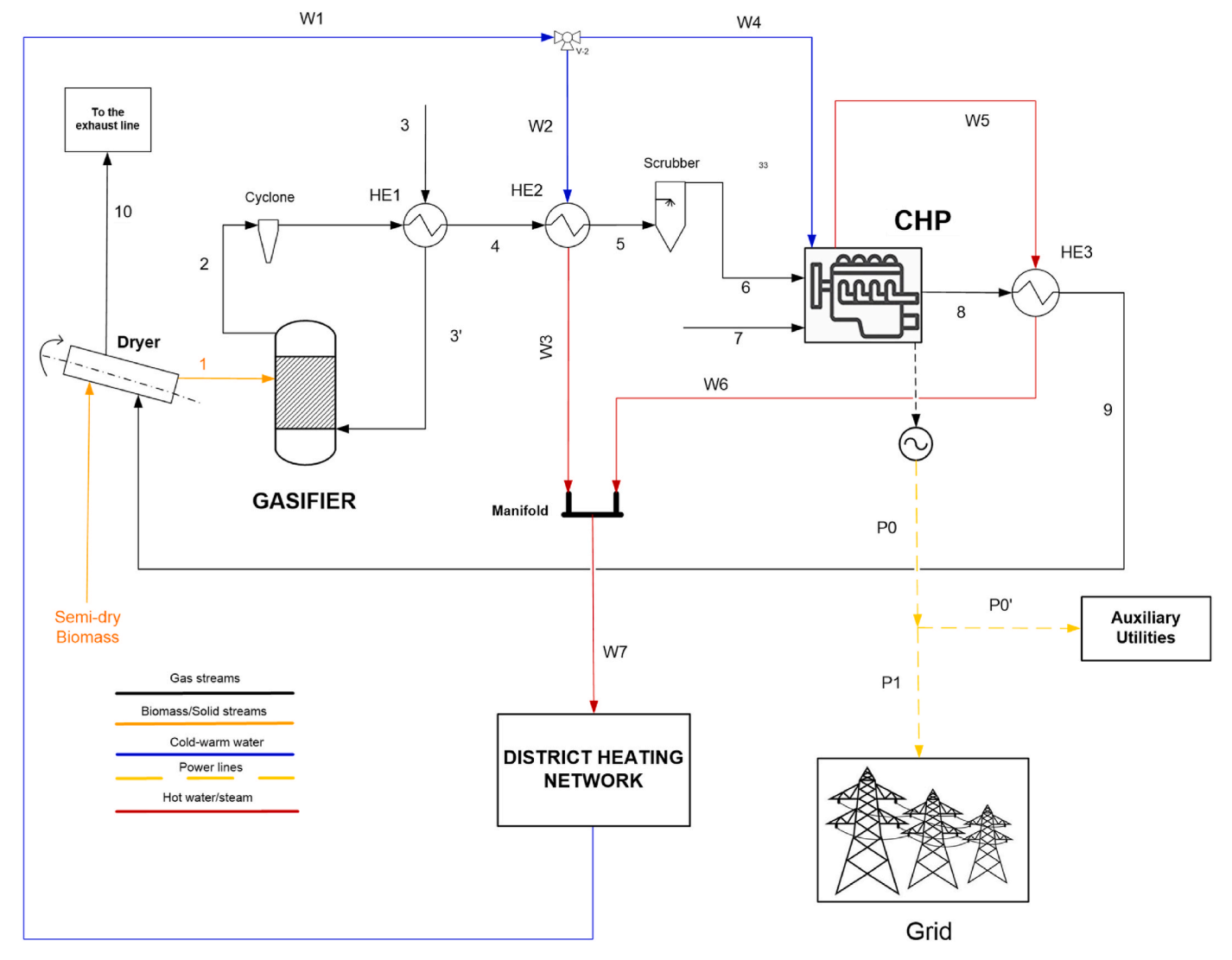


Fig. 3. CHP + DH layout.

temperature is reduced from 200  $^{\circ}$ C to 30  $^{\circ}$ C, without any heat recovery. Hence, in the simulation model, this unit is described by a simple heat exchanger reducing the bio-syngas temperature.

#### 2.4. Combined heat and power (CHP) unit

Another main unit is the combined heat and power unit based on an internal combustion engine. This unit is considered a black box whose net electricity yield is based on the data provided by the constructor (INNIO-Jenbacher). From a preliminary analysis of the possible ranges of syngas yields and heating values, the selected cogeneration model for 1 t/h of feedstock was JMS 612 GS-S.L, which operates given the selected syngas composition (H<sub>2</sub>< 15 % (vol) and 1.4<LHV<1.6 MJ/ Nm<sup>3</sup>). In this unit, low-temperature heat (hot water at 80 °C) is recovered from the intercooler (first stage), lube oil cooling loop, and the jacket water. From the datasheet of the selected cogeneration model, the thermal efficiency of the aforementioned low-temperature heat recovery is 19.64 % (based on the LHV of the bio-syngas). The exhaust gas of the cogeneration unit, which exits the unit at 464  $^{\circ}$ C, yields 3.09 kg per kg of bio-syngas. A fraction of power generated in the CHP unit is considered an internal consumption of the bioenergy system due to ancillary components like screw feeders, pumps, actuators, and others minor equipments, which is assumed to be 15 % of power production from the CHP unit [32]. The main operational assumptions are reported in Table 2.

#### 2.5. Description of the process layouts

As described in section 2.1, two different process layouts of the proposed bioenergy system are analyzed in this work. Fig. 1 shows that the common components are the dryer, the gasifier, and the CHP units, described in the sections above. The two layouts differ in the use of the recovered heat from the syngas cooling and the CHP unit.

At the exit of the gasification reactor, which is operated at 850  $^{\circ}$ C, the temperature of bio-syngas is assumed to be 650  $^{\circ}$ C (after cyclone and the passages along the pipeline to the first heat exchanger). The sensible heat of hot bio-syngas is used at first to heat the gasification agents to 300  $^{\circ}$ C. After this step, further sensible heat recovery is carried out in a second heat exchanger by reducing the bio-syngas to 200  $^{\circ}$ C. This temperature is set as the minimum temperature of bio-syngas to avoid massive tar condensation. From this heat exchanger, which is applied for the second step of heat recovery (HE2 in Figs. 1 and 2), the two process layouts start to differentiate, as described in the following subsections.

#### 2.5.1. Layout CHP + ORC

Fig. 2 shows the process layout of the cogeneration plant according to the CHP + ORC layout. As described above, the heat exchanger HE2 cools down the bio-syngas to 200 °C. In this heat exchanger and for this layout, water from 70 °C to 800 kPa (stream W2) is heated to 170 °C as saturated steam (stream W3). Stream W1, from which streams W2, W4,

W5, and W7 derivate, is the return water of the ORC unit (set at 70 °C). In HE3, sensible heat from the flue gas of the CHP unit (streams 8–9) is transferred to water (streams W7-W8), which is heated at the same conditions as W3. Streams W8 and W3 are then delivered to a manifold that mixes the two streams. The manifold outlet (stream W9), is the high-temperature energy input of the ORC unit as saturated steam at 170 °C. The low-temperature heat recovery in the CHP is obtained by heating water from 70 °C (stream W5) to 80 °C (stream W6). This stream is mixed with stream W10 in the mixing valve of the ORC section, providing additional heat to the low-pressure turbine (LP-T).

The ORC unit considered in this work is a two-stage ORC (also known as dual-loop ORC) to maximize the exploitation of the residual cogenerated heat. It consists of two expanders, two evaporators, and two pumps. Consequently, the cycle works at two different pressure and temperature levels. The organic fluid selected for this work is R-236fa because it was the best-performing fluid modeled by Soffiato et al. [15] in terms of thermal efficiency. The validation of the ORC unit is crucial to guarantee the reliability and replicability of the performance of this unit. The validation of the simulation model of the ORC unit is reported in Table 3, comparing the results of the model developed in AVEVA PRO/II Simulation software with the data of Soffiato et al. [15]. The model of this unit was set by fixing the following according to the reference work: I) the flow rates of the working fluid in the high and low-temperature zones of the unit; II) the temperature of the fluid at the exit of the high and low-temperature evaporators; III) the isoentropic and mechanical efficiencies of turbines and pumps. The other parameters reported in Table 3 are obtained by running the simulation and compared for the model validation. The maximum difference between this model and the data of Soffiato is observed in the output of the high-temperature turbine, which is 4.3 %. However, the thermal efficiency of the whole system is negligible (0.4 %).

The electrical/thermal efficiency of the ORC unit is calculated according to Equation (4), where  $\dot{E}_{H-T,tur}$ ,  $\dot{E}_{L-T,tur}$ ,  $\dot{Q}_{H-T,evap}$ ,  $\dot{Q}_{L-T,evap}$  refer to the actual mechanic work flow of the high and low-temperature turbines, and the heat flow of the high and low-temperature evaporators, respectively.

$$\eta_{th,ORC} = \frac{\dot{E}_{H-T,tur} + \dot{E}_{L-T,tur}}{\dot{Q}_{H-T,evap} + \dot{Q}_{L-T,evap}} \tag{4}$$

After validating the two-stage ORC model based on Soffiato et al. works [15,33], the model was run using the process parameters reported in Table 4.

In the simulation model of the actual ORC unit working for the proposed bioenergy system, the actual flow rate of the organic fluid was calculated by a *Controller* block in the simulation software using the desired temperature (140  $^{\circ}$ C) in stream R2 as the objective function. In HE4, the hot side input is the saturated steam at 170  $^{\circ}$ C (stream W9), which is condensed as saturated liquid (stream W10), while the cold stream is heated and vaporized at 3766 kPa (stream R1, compressed liquid) to 140  $^{\circ}$ C (stream R2, superheated vapor). In HP-T, the organic fluid expands from 3766 kPa to 705 kPa. Stream W10 is mixed with stream W6 (hot water at 80  $^{\circ}$ C and 800 kPa). This stream comes from the

**Table 3** Validation of the ORC unit.

|                               | Soffiato et al. | This work | Difference |
|-------------------------------|-----------------|-----------|------------|
| Heat evaporator low T [kW]    | 5414            | 5598      | 3.4 %      |
| Heat evaporator high T [kW]   | 4360            | 4523      | 3.7 %      |
| Heat condenser [kW]           | 8840            | 9162      | 3.6 %      |
| Low T Turbine inlet[°C]       | 63              | 64        | 1.3 %      |
| Work high T Turbine [kW]      | 395             | 414       | 4.3 %      |
| Work low T Turbine [kW]       | 533             | 542       | 1.7 %      |
| Work low P pump [kW]          | 26              | 26        | 0.0 %      |
| Work high P pump [kW]         | 82              | 82        | 0.5 %      |
| Electrical/Thermal Efficiency | 8.39 %          | 8.38 %    | -0.4 %     |

**Table 4** Assumptions for the ORC unit.

| Parameter   | Value | Units |
|---|-------|-------|
| η <sub>is,PU1</sub> , η <sub>is,PU2</sub> ,                         | 0.70  | [-]   |
| $\eta_{is,HP-T}, \eta_{is,LP-T}$                                    | 0.85  | [-]   |
| $\eta_{m,PU1}$ , $\eta_{m,PU2}$ , $\eta_{m,HP-T}$ , $\eta_{m,LP-T}$ | 0.90  | [-]   |
| ORC Condensing temperature [°C]                                     | 30    | [°C]  |

low-temperature heat recovery unit of the CHP. The mixed stream W11 is directed to HE6 to provide low-temperature heat to the organic fluid (R9), which is heated to 57  $^{\circ}$ C (superheated vapor at 705 kPa). Stream R10 and R3 (HP-T outlet) are at the same pressure (705 kPa) but at different temperatures. They are mixed and directed to the low-pressure turbine (LP-T). Here, the organic fluid expands from 705 kPa to 321 kPa and then condenses at 30  $^{\circ}$ C in HE7. The ORC restarts by increasing the pressure of the liquid to 705 kPa in PU1. A fraction of stream R7 is directed to HE6. The flow rate of R9 is calculated to obtain W1 at 70  $^{\circ}$ C, which is the minimum temperature of the return water into the cogeneration unit. Stream R8 feed pump PU2, which brings the organic fluid to the high-pressure conditions of the cycle (3766 kPa).

#### 2.5.2. Layout CHP + DH

Fig. 3 shows the process layout where the net cogenerated heat is used in the district heating network (DH). In this layout, heat from biosyngas cooling is recovered as hot water at 93 °C and 300 kPa (W3). In the CHP unit, a fraction of the return water from the DH is directed to the low-temperature heat recovery, and then it receives heat from the flue gas of the engine (at 464 °C) in the heat exchanger HE3 to reach the same conditions of stream W3. As for the previous layout, the flue gas is cooled in the range 150–170 °C. After this heat recovery step, W6 is mixed with W3. Then, the mixed stream W7 represents the energy input of the DH network. The global heat loss from the district heating is assumed to be 20 % of the gross available heat (considering 93°C–70 °C as the temperature variation of stream W7 [34]. The thermodynamic parameters and the flow rates of each stream are listed in the results section because most of them are the results of the simulation model.

#### 2.6. Process analysis

The thermal  $(Y_{th})$  and electrical  $(Y_{el})$  energy yields are calculated for both process layouts as the net electricity and net thermal energy, after internal consumptions, per unit of biomass (MJ/kg<sub>db</sub>).

$$Y_{el} = \frac{E_{el}}{m_{blow, ph}} \tag{5}$$

$$Y_{th} = \frac{E_{th}}{m_{biom\_db}} \tag{6}$$

The energy and the exergy analysis of the two layouts were carried out for each main unit and at a global level by assessing the energy and exergy efficiencies for the whole process.

For each stream of the of the two layouts, the exergy has been calculated as the sum of physical  $(E_{ex}^{ph})$  and chemical exergy  $(E_{ex}^{ch})$ , ignoring the variations of kinetic and potential exergy.

Consequently, the exergy of a material stream is calculated as:

$$E_{ex} = E_{ex}^{ph} + E_{ex}^{ch} \tag{7}$$

The physical exergy is defined according to the following equation [17]:

$$E_{ex}^{ph} = \dot{m}[h - h_0 - T_0(s - s_0)] \tag{8}$$

where the subscript "0" refers to thermodynamic variables at the reference state (20  $^{\circ}$ C and 101 kPa in this work).

The chemical exergy of a stream is calculated as [17]:

$$E_{ex}^{ch} = \dot{m} \left( \sum_{i} x_{i} e_{x,i}^{ch} + RT_{0} \sum_{i} x_{i} \ln x_{i} \right)$$
 (9)

Where  $x_i$  is the concentration of the i substance,  $e_{x,i}^{ch}$  is the specific chemical exergy of the i substance. The specific chemical exergy of each substance involved in this work was obtained from Bakshi et al. [16].

The exergy exchange  $(E_{ex}^Q)$  due to a heat transfer  $Q_i$  is calculated as it follows:

$$E_{\rm ex}^{\rm Q} = Q_i \left( 1 - \frac{T_i}{T_0} \right) \tag{10}$$

Where  $T_i$  is the temperature at the control surface where heat transfer is taking place.

The chemical exergy of biomass is calculated according to the following equation based on the high heating value on a dry basis  $(HHV_{db})[12]$ :

$$e_{x \, biomass}^{ch} = 1.047 \bullet HHV_{db} \tag{11}$$

The exergy/energy ratio of electricity is assumed as 1.

Energy and exergy efficiencies of the cogeneration plant are assessed according to the following equations:

$$\eta_{en\_global} = \frac{\dot{E}_{elCHP} + \dot{E}_{elORC} + \dot{E}_{DH}}{\dot{E}_{biom}}$$
 (12)

$$\eta_{ex\_global} = \frac{\dot{E}_{ex\_elCHP} + \dot{E}_{ex\_elORC} + \dot{E}_{ex\_DH}}{\dot{E}_{ex\_biom}}$$

Where  $\dot{E}_{elCHP}$ ,  $\dot{E}_{elORC}$ ,  $\dot{E}_{DH}$ , and  $\dot{E}_{biom}$  are the net electricity output from the cogeneration unit, from the ORC unit (in the CHP + ORC layout), the district heat (in the CHP + DH layout), and the chemical energy input from biomass, respectively. The subscript ex refers to the exergy values of the homologous energy streams mentioned above.

As described in the previous sections, electricity generation in the CHP unit is modeled on the net electrical efficiency ( $\eta_{elCHP}$ , see Table 2) of the selected cogeneration system designed for bio-syngas as input fuel, the lower heating value ( $LHV_{syn}$ ) and the mass flow rate ( $\dot{m}_{syn}$ ) of syngas, as expressed in the following equation:

$$\dot{E}_{elCHP} = \eta_{elCHP} \bullet LHV_{syn} \bullet \dot{m}_{syn} \tag{13}$$

The net electricity output from the ORC unit ( $E_{elORC}$ ), which is indicated in Equation (11), is calculated as the sum of the work produced by the high ( $\dot{E}_{HP-T}$ ) and low pressure ( $\dot{E}_{LP-T}$ ) turbines subtracted by input work required by the high ( $\dot{E}_{PU2}$ ) and low pressure ( $\dot{E}_{PU1}$ ) pumps, as reported in Eq. (14).

$$\dot{E}_{elORC} = \dot{E}_{HP-T} + \dot{E}_{LP-T} - \dot{E}_{PU1} - \dot{E}_{PU2} \tag{14}$$

The data on work for pumps and turbines are obtained from the simulation model and are based on the assumed isentropic and mechanical efficiencies reported in Table 4.

Rational efficiency and irreversibility were used as performance parameters to assess the exergy efficiency of each unit. Rational efficiency is defined as the ratio between the exergy variation of the desired output and the exergy variation of the necessary input [17]:

$$\eta_{rational} = \frac{\sum \Delta E_{ex\_out}}{\sum \Delta E_{ex\_in}}$$
 (15)

where  $\Delta E_{ex\_in}$  and  $\Delta E_{ex\_out}$  are the exergy transfer making the input and the output, respectively.

In the case of heat exchangers, the definition of the numerator and denominator is almost straightforward. The desired output is the increase or reduction of the temperature of the target stream we want to heat up or cool down, while the input is the exergy variation of the other

stream. In the case of the gasifier, the numerator is the difference between the bio-syngas exergy and gasifying agents as the desired process output, while the input is the dry biomass. Contrarily to the equation of rational efficiency proposed by Ptasinski for gasifiers [12], in this case, the exergy of the solid residue is neglected. For the power generation unit, the numerator of the rational efficiency consists of the gross power, the increase in exergy content of water (from the return to the supply water) after exchanging heat with hot exhaust gas, summed to the residual exergy of exhaust gas, which is cooled down to 160 °C to be used in the dryer. The exergy variation of the input (denominator) consists of the fuel exergy. From the above, it follows that in this work the rational efficiency of the cogeneration unit includes the heat recovery from the engine and the exhaust gas. The exploitation of the residual exergy of the exhaust gas is computed in the exergy efficiency of the dryer. In gas turbines, the rational efficiency is calculated using the exergy variation of the working fluid as the denominator, while the numerator is the power output. In addition to the rational efficiency of the single devices constituting the ORC unit, the rational efficiency of the ORC as a whole has been calculated. In this case, the desired output is the net power production from the two turbines. At the same time, the necessary input is represented by the exergy variation between the hot-water streams considered as input, stream W6 and stream W9, and the exiting return water stream (W1).

#### 2.6.1. Considering the following exergy balance

$$\sum \Delta E_{ex\_in} = \sum \Delta E_{ex\_out} + I \tag{16}$$

where *I* stands for the irreversibility of the process under examination, it is possible to use the following equation calculate the irreversibility of each main unit.

$$I_{i} = \left(1 - \eta_{rational,i}\right) \bullet \sum \Delta E_{ex_{in,i}} \tag{17}$$

The contribution of each component  $(I_i)$  to the overall irreversibilities  $(I_{overall})$  of a process can be analyzed by calculating the relative irreversibility (r):

$$r = \frac{I_i}{I_{overall}} \tag{18}$$

$$I_{overall} = \sum I_i \tag{19}$$

The irreversibility indicated above includes both internal and external irreversibilities. External irreversibility is defined as the lost exergy, as in the case of exhaust gas, which exists at the system boundary at a temperature higher than the reference state. This is also known as exergy loss or avoidable irreversibility. Therefore, internal irreversibility is related to the nature of the process and the variation of entropy, also called exergy destruction.

The sustainability index (SI) is the ratio of the fuel exergy to the overall irreversibility [35]. The higher the exergy loss and the exergy destruction, the lower the index's sustainability when compared to the amount of exergy introduced with the fuel. This index describes how a resource (in this case, biomass) is used sustainably from a thermodynamic point of view.

$$SI = \frac{E_{ex\_fuel}}{I_{overall}} \tag{20}$$

Another important exergy-based indicator is the exergy improvement potential (EIP), which can be calculated for each process unit [36]. This indicator is directly proportional to the irreversibility. Consequently, the process or unit with the highest irreversibility has the maximum opportunity to improve the exergetic performance of the system [35]. As it can be noted from the following equation of EIP, as the rational efficiency increases, the potential for performance improvement reduces.

$$EIP_i = (1 - \eta_{rational.i}) I_i \tag{21}$$

## 3. Results and discussion

M. Prestipino et al.

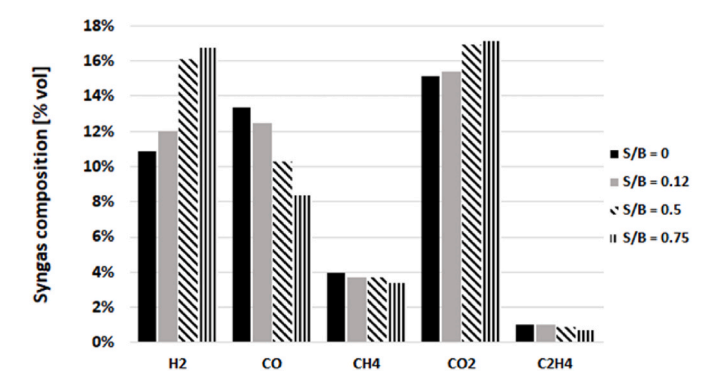
The simulation models were based on the experimental results of reed gasification, as described in the methods section. Specifically, the input stream of the model is a syngas stream with a composition and flow rate that was selected according to the following results.

Fig. 4 shows the bio-syngas composition obtained at different steam-to-biomass ratios (S/B), ranging from 0 to 0.75, fixed equivalence ratio (ER = 0.3), and reactor temperature of 850  $^{\circ}$ C. As expected, the hydrogen concentration increases as the steam flow increases. Similarly, carbon dioxide increases with steam, while carbon monoxide decreases. This behavior may be associated with the progress of the water-gas shift reaction, favored by the increased water flow rate. Hydrocarbons slightly reduce as the S/B increases due to steam-reforming reactions.

The reduction in hydrocarbons and carbon monoxide concentration reduced the heating value of the bio-syngas, which is partially compensated by the higher hydrogen formation. Fig. 5 shows the variation of bio-syngas heating value, yield, and cold gas efficiency with the S/B parameter.

The bio-syngas yield shows minor variations (2.14–2.19 Nm<sup>3</sup>/kg<sub>db</sub>) when the steam-to-biomass ratio varies from 0 to 0.5. When S/B is increased to 0.75, the yield rises more clearly to 2.36 Nm<sup>3</sup>/kg<sub>db</sub>. The lower heating value (LHV) trend is very flat until S/B = 0.5 (4.92-4.91  $MJ/Nm^3$ ) while at S/B = 0.75 a more evident reduction is observed (4.54 MJ/Nm<sup>3</sup>). The reduction of the LHV with S/B is consistent with the variation of the syngas composition where methane (LHV = 35.88 MJ/ Nm<sup>3</sup>) and carbon monoxide (LHV = 12.63 MJ/Nm<sup>3</sup>) decrease, while hydrogen (LHV =  $10.78 \, \text{MJ/Nm}^3$ ) and carbon dioxide increase with S/B. It follows that the reduction of methane and carbon monoxide concentrations is not compensated by hydrogen in terms of LHV. This behavior is attributed to the progression of the steam-carbon, water-gas shift, and reforming reactions when the S/B increases, which also explains the slight increase of the bio-syngas yield. Indeed, as the reactions mentioned above are favored, the bio-syngas and hydrogen yields increase. In terms of cold gas efficiency (CGE), the performance of the gasification process is almost constant, showing a flat trend in the entire range of S/B, varying from 0.60 to 0.61. This behavior is consistent with the LHV decreasing while the bio-syngas yield increases. The negligible impact of the steam-to-biomass ratio on the syngas yield should be attributed to the presence of silica in the inorganic fraction of the feedstock, which has an inhibition effect on the steam-char reaction [37]. A possible solution to minimize this effect and increase the syngas yield with the S/B is the use of Ca-based or K-based inorganic catalyst as bed material of the reactor [37].

Due to the lack of comparable literature data on Arundo Donax gasification, the CGE can be compared with a similar feedstock. Couto et al. [38] analyzed the performance of Miscanthus gasification by using



**Fig. 4.** Bio-syngas composition obtained by Arundo Donax gasification at different S/B values.

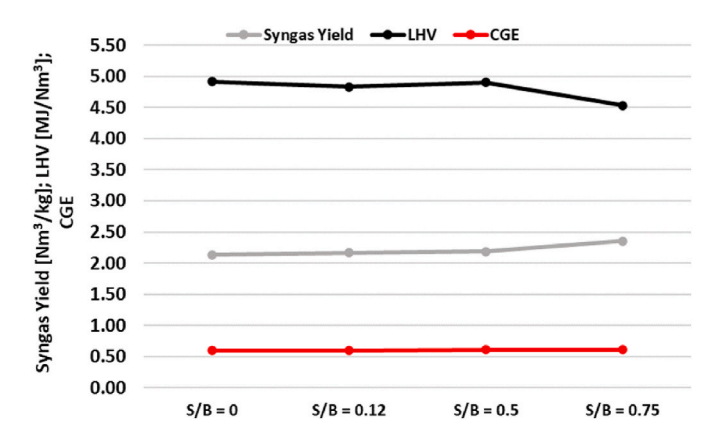


Fig. 5. Performance of Arundo Donax gasification.

a bubbling fluidized bed gasifier. They found out that the CGE of air and air/steam gasification was between 0.58 and 0.63, as the S/B varies from 0 to 0.5, which is in the range of the results obtained for the Arundo Donax in this work. As studied in this work, this feedstock shows a slight influence from using steam as a gasification medium in terms of CGE. Indeed, as reported by Ge et al. [39], Arundo Donax and Miscanthus are considered competitive energy crops because both can lead to similar energy yields per unit of dry feedstock.

Considering that the variation in the CGE is negligible, that the heating value decreases as the steam flow increases, and that the biosyngas is delivered into an internal combustion engine, the gasification condition selected in this work for the process simulation and integration is S/B=0. Hence, the only gasification agent used in this work is air. Avoiding the use of steam involves an additional simplification of the whole process.

As a result of the process simulation of the proposed process layouts, the thermodynamic properties of the main streams for the layout CHP + DH are reported in Table 5, in which the stream numbers are referred to those in Fig. 3. The main energy and exergy output flows considered are reported in Table 6. All results are referred to 1 t/h of biomass on a dry basis. The latter table shows that the net electrical energy yield is 0.922 MWh/t<sub>db</sub> (P1), while the net thermal energy yield (DH net) is 1.316 MWh/t<sub>db</sub>. The difference between the gross (DH gross) and the net thermal energy is the thermal energy loss in the district heating network (DH loss), which is assumed to be 20 % of the DH gross. In Table 6, PO and P0' are the electrical power production from the cogeneration unit and power consumption of the auxiliary units, respectively. Compared to the output reported by Nguyen et Hermansen for energy production from Miscanthus (a biomass of a similar origin and similar characteristics of giant reed) [40], the electrical energy yield obtained in this work is 40 % smaller. On the other side, confronting this work with the results of Allesina et al. regarding Giant Reed gasification into a micro-scale fixed bed gasifier [41], the electricity yield reported in this work is about 150 % higher. However, Allesina et al. used a fixed bed gasifier and a micro-scale internal combustion engine, which is affected by low energy conversion efficiency [42]. Unfortunately, the literature review revealed that there are no direct comparable data for power production fed by the feedstock that is the object of this work, so literature data need to be adapted for comparison. Although this aspect limits the possibility of comparing the results of this work with the available literature, it represents the main motivation of this work and underlines its relevance and novelty. Aiming to compare the reported results with other technologies used for Arundo Donax energy conversion described in the literature, Soleimani et al. [41] recently reported that the potential biomethane yield from Arundo Donax in anaerobic digestion is about 0.174 Nm<sup>3</sup>/kg, which leads to potential power production in the range 0.63-0.65 MWh/t, assuming 36.8 % of electrical efficiency in the cogeneration unit. This electricity yield is just 70 % of the net electricity

Table 5 Thermodynamic properties of the main streams for layout CHP + DH (1 t/h of biomass on a dry basis).

| Stream           | Flow Rate [kg/s] | Temperature [°C] | Pressure [kPa] | Specific Heat [kJ/kgK] | Enthalpy [kJ/s] | Entropy [kJ/sK] | Exergy [MJ/s] |
|------------------|------------------|------------------|----------------|------------------------|-----------------|-----------------|---------------|
| Evaporated water | 0.039            | 90               | 101            | 4.187                  | 11.69           | 0.04            | 0.085         |
| Semi dry biom    | 0.347            | 20               | 101            | 2.000                  | NA              | NA              | 5.448         |
| 1                | 0.309            | 20               | 101            | 2.000                  | NA              | NA              | 5.456         |
| 2                | 0.718            | 650              | 101            | 1.378                  | 630.43          | 6.17            | 3.231         |
| 3                | 0.307            | 20               | 120            | 1.016                  | -2.30           | 1.97            | 0.000         |
| 3'               | 0.307            | 300              | 140            | 1.054                  | 87.72           | 2.18            | 0.032         |
| 4                | 0.718            | 558              | 140            | 1.345                  | 540.42          | 6.07            | 3.171         |
| 5                | 0.718            | 200              | 140            | 1.205                  | 212.82          | 5.56            | 2.994         |
| 6                | 0.718            | 30               | 110            | 1.138                  | 69.86           | 5.19            | 2.960         |
| 7                | 1.500            | 20               | 200            | 1.018                  | -3.93           | 9.43            | 0.000         |
| 8                | 2.218            | 464              | 140            | 1.155                  | 1436.33         | 16.32           | 1.310         |
| 9                | 2.218            | 164              | 140            | 1.142                  | 1331.73         | 16.17           | 1.248         |
| 10               | 2.218            | 120              | 140            | 1.060                  | 593.43          | 14.79           | 0.916         |
| W1               | 17.250           | 70               | 300            | 4.187                  | 5058.32         | 16.47           | 1.144         |
| W2               | 3.450            | 70               | 300            | 4.187                  | 1011.66         | 3.29            | 0.229         |
| W3               | 3.450            | 93               | 300            | 4.180                  | 1339.26         | 4.22            | 0.286         |
| W4               | 13.800           | 70               | 300            | 4.187                  | 4046.66         | 13.18           | 0.915         |
| W5               | 13.800           | 80               | 300            | 4.187                  | 4625.66         | 14.84           | 1.007         |
| W6               | 13.800           | 93               | 300            | 4.180                  | 5363.95         | 16.89           | 1.144         |
| W7               | 17.250           | 93               | 300            | 4.180                  | 6703.21         | 21.11           | 1.429         |

Table 6 Main energy and exergy flows for layout CHP + DH (1 t/h of biomass on a dry basis).

| Stream            | P0    | P0'   | P1    | DH<br>gross | DH<br>net | DH<br>loss |
|-------------------|-------|-------|-------|-------------|-----------|------------|
| Power/Heat flow   | 1.085 | 0.163 | 0.922 | 1.645       | 1.316     | 0.329      |
| Exergy Flows [MW] | 1.085 | 0.163 | 0.922 | 0.285       | 0.228     | 0.057      |

yield obtained in the cogeneration unit of this work. According to Ceotto et al. [43] the anaerobic digestion of Arundo Donax leads to 0.45–0.74 MWh/t under the same engine's electrical efficiency. The reason for the larger energy yield of thermochemical gasification compared to anaerobic digestion lies in the nature of the two processes, thermochemical and biochemical, respectively. In the first one, the carbon conversion is very high thanks to the high temperature and the use of gasification agents. At the same time, the digestate still has a considerable amount of unconverted organic matter.

Table 7 and Table 8 show the primary material and energy streams for the layout of CHP + ORC (see Fig. 2). This layout has no net available

 $\label{thm:continuous} \textbf{Table 7} \\ \textbf{Thermodynamic properties of the main streams for layout CHP} + \textbf{ORC (1 t/h of biomass on a dry basis)}.$ 

| Stream           | Flow Rate [kg/s] | Temperature [°C] | Pressure [kPa] | Specific Heat [kJ/kgK] | Enthalpy [kJ/s] | Entropy [kJ/sK] | Exergy [MJ/s] |
|------------------|------------------|------------------|----------------|------------------------|-----------------|-----------------|---------------|
| Evaporated water | 0.039            | 90               | 101            | 4.19                   | 11.69           | 0.04            | 0.081         |
| Semi dry biom    | 0.347            | 20               | 101            | 2.00                   | NA              | NA              | 5.448         |
| 1                | 0.309            | 20               | 101            | 2.00                   | NA              | NA              | 5.456         |
| 2                | 0.718            | 650              | 101            | 1.38                   | 630.43          | 6.17            | 3.231         |
| 3                | 0.307            | 20               | 101            | 1.02                   | -2.30           | 1.97            | 0.000         |
| 3'               | 0.307            | 300              | 140            | 1.05                   | 87.72           | 2.18            | 0.032         |
| 4                | 0.718            | 558              | 140            | 1.35                   | 540.42          | 6.07            | 3.171         |
| 5                | 0.718            | 200              | 140            | 1.20                   | 212.82          | 5.56            | 2.994         |
| 6                | 0.718            | 30               | 110            | 1.14                   | 69.86           | 5.19            | 2.960         |
| 7                | 1.500            | 20               | 101            | 1.02                   | -3.57           | 9.72            | 0.000         |
| 8                | 2.218            | 464              | 140            | 1.15                   | 1436.33         | 16.32           | 1.310         |
| 9                | 2.218            | 167              | 140            | 1.14                   | 1331.73         | 16.17           | 1.248         |
| 10               | 2.218            | 122              | 140            | 1.06                   | 593.43          | 14.79           | 0.916         |
| W1               | 14.249           | 70               | 800            | 4.19                   | 4184.00         | 13.60           | 0.952         |
| W2               | 0.130            | 70               | 800            | 4.19                   | 38.87           | 0.13            | 0.009         |
| W3               | 0.130            | 170              | 800            | 2.60                   | 366.47          | 0.88            | 0.115         |
| W4               | 14.124           | 70               | 800            | 4.19                   | 4145.13         | 13.47           | 0.944         |
| W5               | 13.818           | 70               | 800            | 4.19                   | 4057.52         | 13.19           | 0.923         |
| W6               | 13.818           | 80               | 800            | 4.19                   | 4636.00         | 14.85           | 1.015         |
| W7               | 0.306            | 70               | 800            | 4.19                   | 87.61           | 0.28            | 0.020         |
| W8               | 0.306            | 170              | 800            | 2.60                   | 825.90          | 1.99            | 0.260         |
| W9               | 0.436            | 170              | 800            | 2.60                   | 1192.37         | 2.87            | 0.375         |
| W10              | 0.436            | 170              | 800            | 4.37                   | 311.54          | 0.88            | 0.076         |
| W11              | 14.254           | 83               | 800            | 4.20                   | 4948.04         | 15.79           | 1.076         |
| R1               | 4.418            | 33               | 3766           | 1.27                   | 185.99          | 20.60           | 0.060         |
| R2               | 4.418            | 140              | 3766           | 2.46                   | 1066.82         | 23.00           | 0.238         |
| R3               | 4.418            | 75               | 705            | 0.96                   | 977.50          | 23.05           | 0.135         |
| R4               | 9.030            | 66               | 705            | 0.96                   | 1920.63         | 46.88           | 0.265         |
| R5               | 9.030            | 48               | 321            | 0.89                   | 1823.71         | 46.93           | 0.152         |
| R6               | 9.030            | 30               | 321            | 1.29                   | 346.98          | 42.08           | 0.097         |
| R7               | 9.030            | 30               | 705            | 1.29                   | 350.68          | 42.08           | 0.100         |
| R8               | 4.418            | 30               | 705            | 1.29                   | 171.59          | 20.59           | 0.049         |
| R9               | 4.611            | 30               | 705            | 1.29                   | 179.09          | 21.49           | 0.051         |
| R10              | 4.617            | 57               | 705            | 0.95                   | 943.13          | 23.83           | 0.138         |

thermal energy because it is used for power production in an ORC unit. Indeed, the residual heat from the ORC unit is discarded since it is a very low-enthalpy heat flow. The net power yield from the cogeneration unit is the same as in the other scenario. However, the global net electricity yield is 1.069 MWh/t<sub>db</sub>, 16 % higher than the CHP + DH layout. Comparing the total net exergy output, the mentioned tables show that layout CHP + DH is 1.151 MWh/t<sub>db</sub>, while it is 1.069 MWh/t<sub>db</sub> in layout CHP + ORC. In relative terms, the CHP + DH layout can generate about 8 % more net exergy output. This result shows that the low energy yield of the ORC unit negatively compensates for the high-quality energy output obtained from the conversion of heat into electricity.

From the research work of Alexopoulou et al. [44], it turns out that the average giant reed yield as an energy crop is  $15.6\,\mathrm{t/ha}$ , in a scenario with scarce irrigation and no fertilization. By combining this data with the availability of marginal lands in Sicily (Italy), which is 424,700 ha (according to the results of the MAGIC h2020 European project [45]), the additional renewable electrical energy production in the region could be about 610–710 GWh/year (depending on the process layout) if only 10 % of marginal lands in Sicily were exploited to cultivate giant reed as an energy crop. The mentioned production equals about 10 % of the region's existing renewable electrical energy production. Considering the invasive nature of giant reed in the Mediterranean areas (it is regarded as a weed in many places), the renewable energy production in the region could be even higher if the availability of giant reed from land management were quantified.

Fig. 6 shows the rational efficiencies of the main units of the two process configurations. As from the equation of the rational efficiency reported in section 2, this efficiency describes the capacity of the analyzed process to convert the exergy variation of the necessary input streams into the desired exergy variation as output.

For both process layouts, the highest rational efficiency is observed for the cogeneration unit, which includes a partial heat recovery from the engine and the exhausts (units CHP and H3 in Figs. 2 and 3). Furthermore, the rational efficiency of the cogeneration unit includes the residual heat of exhaust gas as an output. Without this contribution, the rational efficiency would drop from 0.86 to 0.44. The way the exergy of this residual stream is used is considered in the energy/exergy analysis of the drying unit since this is the unit where part of the residual exergy of the flue gas is used. This unit shows the lowest rational efficiency (0.01). Such a low efficiency is typical of those processes occurring naturally, as described by Kotas [17]. Another reason for such low exergy efficiency is the loss of exergy caused by the mixing of the residual exhaust gas with the environment. For the CHP + DH layout, the district heating network (DH) has the second highest rational efficiency. In this work, the DH is simulated as a heat exchanger where water is cooled from 93  $^{\circ}$ C to 70  $^{\circ}$ C (return water temperature), 20 % of the heat is lost [34], and the heat is exchanged at an average temperature of 81.5  $^{\circ}$ C. Consequently, the net available heat is the difference between the gross heat and the heat loss. The exergy of this net heat flow is then divided by the exergy variation of water from streams W7 and W1 (gross heat). The rational efficiency of the gasification unit is 0.59 for both process layouts since this process is the same in the two layouts. The performance of the gasifier in this work could be improved by further optimization of the process conditions since the rational efficiency is low for this unit, which is in agreement with the research work by Prins et al. [46]. This result is a consequence of the low cold gas efficiency described above.

Regarding the whole ORC unit, the rational efficiency is 0.34, which is in the range of the values presented by Sun et al. [47]. In terms of energy efficiency, this unit showed a value of 0.09, in accordance with

Table 8 Main energy flows for layout CHP + ORC (1 t/h of biomass on a dry basis).

|  |            |       | •     |       | •     |       |       |       |
|--|------------|-------|-------|-------|-------|-------|-------|-------|
|  | Stream     | P0    | P0'   | P1    | P2    | P2'   | Р3    | P3'   |
|  | Power [MW] | 1.085 | 0.163 | 0.922 | 0.064 | 0.016 | 0.083 | 0.004 |

the simulation model of Soffiato et al. [15,33].

Fig. 7 presents the relative irreversibilities for the two process layouts, considering the main components. As expected, the gasification unit has the highest relative irreversibility, reaching about 50 % of the total (53 % and 51 % in CHP + DH and CHP + ORC, respectively). This can be explained considering that, in this unit, the main exergy input is converted into another physical state, which involves the highest exergy flow crossing a single unit. This result is comparable to those reported by Ptasinski [12]. The second contribution to the irreversibility of the whole process is the drying unit, which is a consequence of the very low rational efficiency described above. The CHP unit covers about 9 % of the relative irreversibility in layout CHP + DH, while this value reaches about 7 % in layout CHP + ORC. It is important to note that the low relative irreversibilities of the CHP unit are because the whole exergy content of the flue gas is considered one of the outputs. If only the exergy of the flue gas actually used were included in the CHP rational efficiency instead of the total amount of its exergy, the relative irreversibility would be in the range of 20-22 %. In this work, the actual exergy variation of the flue gas is taken into account in the drying unit. Hence, the quality of the conversion and use of this stream is considered downstream and in the rational efficiency of the whole process, as described below in this section.

The differences in the relative irreversibilities for the two layouts are due to the additional irreversibilities introduced by the ORC process. The contribution of the different units of the ORC section to the irreversibility of the whole process is about  $2\,\%$ .

Regarding the district heating, the irreversibilities are mainly due to external exergy loss due to the assumption that 20 % of the energy content of the hot water stream is lost as heat transfer to the atmosphere [34].

Fig. 8 shows the Exergy Improvement Potential (EIP), describing the potential improvements that can be made for each process component. For both scenarios, the most significant improvements can be made in the dryer. The high EIP of the dryer is related to the significant exergy loss at low temperatures and the very low rational efficiency, as explained above. A possible approach to improve the EIP is the implementation of a low-temperature waste heat recovery system, which is still an open challenge for efficiency improvement in the industrial sector [48]. A second relevant source of EIP is the gasifier due to the high irreversibility production, as reported by Sinha et al. [35]. In this work, the large EIP, exergy loss, and irreversibility of the gasifier are also consequences of the low cold gas efficiency reported for the gasification of Arundo Donax in Fig. 5.

From the initial input of 5.45 MW (considering 1 t/h of feedstock on a dry basis), the total irreversibility generated by the proposed process is 4.3 MW for CHP + DH and 4.4 MW for CHP + ORC, as reported in Fig. 9. The same figure shows the Sustainability Index, which indicates how much of the fuel's exergy (biomass) is not lost as irreversibility. The higher the sustainability index, the lower the amount of fuel's exergy converted into irreversibility. Since the fuel's exergy input is the same for the two process layouts, in this study, the sustainability index and the irreversibility show the same differences between the two scenarios. Indeed, the CHP + ORC layout generates just 2 % more irreversibility and 2 % less sustainability index than the CHP + DH process layout.

This leads to a slightly higher exergy efficiency for the process layout CHP + DH compared to the CHP + ORC, as shown in Fig. 10. This figure shows that the energy efficiency of the two processes is very different, with the CHP + DH layout performing 109 % better than the CHP + ORC layout (46 % and 22.0 %). The significant difference in the global energy efficiency between the two layouts is due to the very low energy efficiency of the ORC cycle in converting heat into electricity. In this work, the energy efficiency of the ORC cycle is 8.9 %. Regarding the electrical efficiencies of the proposed layouts (19 % and 22 % for the CHP + DH and CHP + ORC layouts, respectively), these are lower than those of the well-renowned Gussing and Viking gasification-CHP plants, which are about 25 % [49]. In terms of overall gross energy efficiency (i.e.,

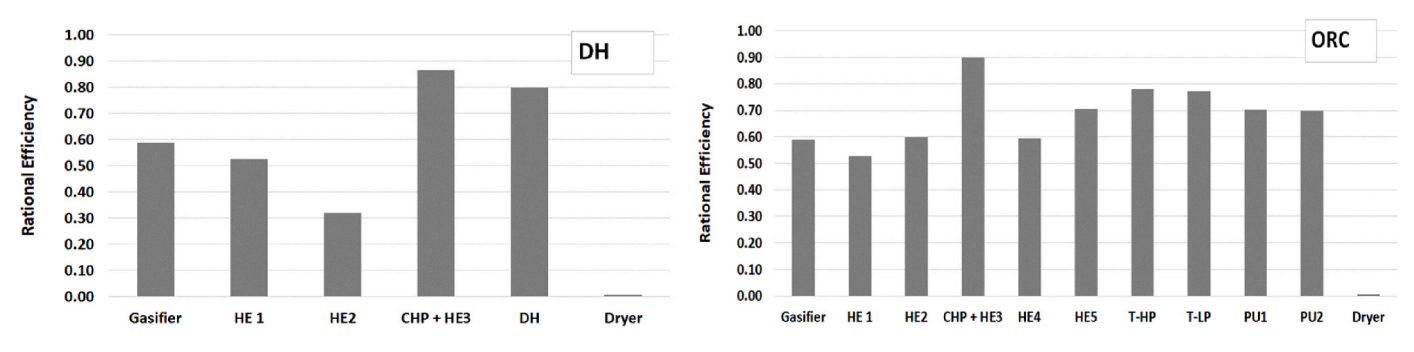


Fig. 6. Rational efficiencies of the main components of the two process layouts.

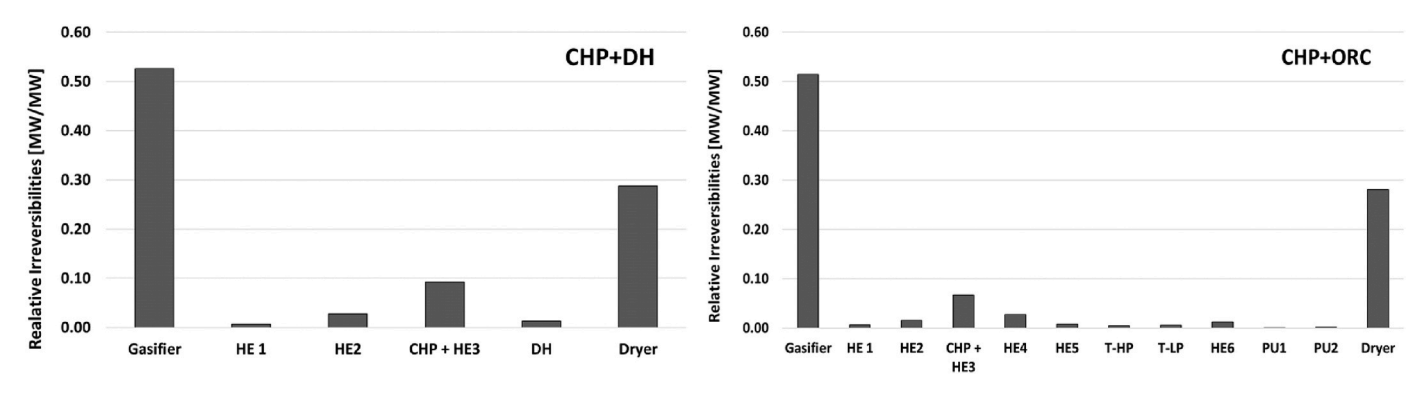


Fig. 7. Relative irreversibilities of the proposed process layouts.

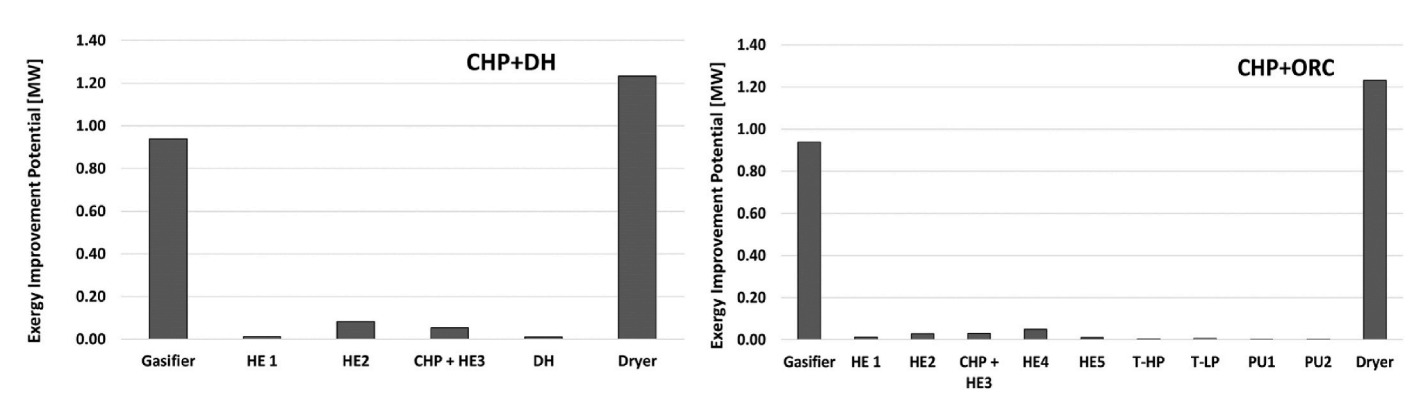


Fig. 8. Exergy Improvement Potential for the investigated process layouts.

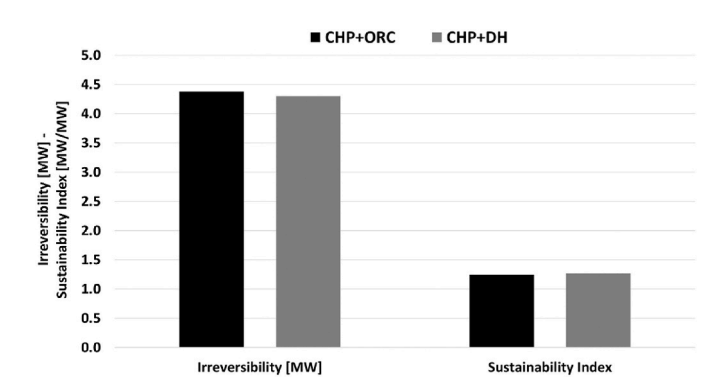


Fig. 9. Irreversibility and Sustainability Index of the two process layouts.

including the cogenerated heat used in the drying unit and not considering the heat loss in the DH network), the CHP + DH layout shows 81 % energy efficiency, which is comparable to those obtained in the

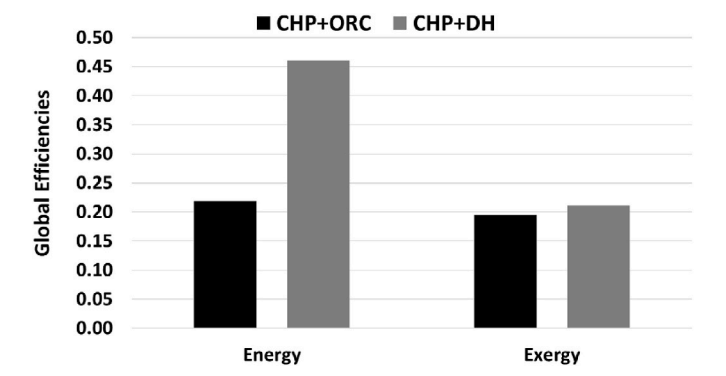


Fig. 10. Energy and exergy efficiencies of the whole process for the two layouts.

above-mentioned plants [49]. However, Gussing and Viking CHP systems are fed by wood, which usually generates higher syngas yield than other feedstocks. Furthermore, these two plants have gasification reactor designs different from the one presented in this work. From the point of view of global exergy efficiency, the differences between the two investigated layouts are much less marked than in the case of energy efficiency. Indeed, the CHP + DH layout shows exergy efficiency just 5% higher than the CHP + ORC scenario. This reduced difference is due to the higher energy quality of the energy product (electricity) in the case of ORC. Hence, it is evident that the higher quality of energy output in the CHP + ORC layout compensates for the low energy yield of this kind of heat utilization. Consequently, the differences between the two process layouts are minimal in terms of thermodynamic quality or thermodynamic sustainability of resource exploitation, especially regarding irreversibility and sustainability index (2%).

#### 4. Conclusions

This research develops a comprehensive and comparative performance assessment of a cogeneration/combined cycle process based on Arundo Donax (Giant Reed) gasification analyzing two different process layouts that differ in the use of the cogenerated heat. In one layout, the cogenerated heat is used in a district heating network, while in the other layout, heat powers an Organic Rankine Cycle (ORC). The bioenergy system is based on Arundo Donax gasification's original and new experimental data presented in this work. Then, process simulations are carried out. The primary outcomes determined for 1 t/h of feedstock (dry basis) can be summarized as follows.

- ✓ In the scenario CHP + DH (with combined cogeneration and district heating), the net power output is 0.922 MW, while the net heat available to the district heating network users is 1.316 MW.
- $\checkmark$  In the scenario CHP + ORC (cogeneration and ORC), the net power output is 1.069 MW.
- ✓ The highest rational efficiency is observed in the cogeneration unit (which includes heat from the exhaust gas), while the highest contribution to the relative irreversibilities is due at first to the gasifier and secondly to the dryer. These results are valid for both layouts.
- ✓ The global energy efficiencies are 0.46 and 0.22 for CHP + DH and CHP + ORC layouts, respectively, while the exergy efficiencies are minimal (0.21 vs 0.20).
- ✓ The amount of irreversibility generated in the CHP + ORC scenario is 2 % higher than the CHP + DH scenario, which leads to 2 % lower irreversibility.
- ✓ Similarly, the Sustainability Index of the CHP + ORC scenario is 2 % lower than the CHP + DH scenario.

#### 4.1. Key points and implications

Despite the expected higher energy efficiency of the CHP + DH layout (cogeneration and district heating), the results of the exergy efficiencies show that the differences between the two scenarios are much less than those related to energy (5 % vs. 52 %). Along with the differences in the Sustainability Index (2 %), the main implication of these results is that the two layouts show negligible differences in the sustainable use of the resources according to a thermodynamic analysis based on the second principle. This approach leads to conclusions different from those drawn from process analysis based on energy data instead of exergy. In conclusion, it can be stated that, from the thermodynamic point of view, the sustainability of the two processes is comparable. It follows that the final decision to adopt one or the other process layout should be based not only on the economic and environmental analyses, which are affected by the specific context where the system is integrated but also on the thermodynamic sustainability of the

processes. The comparative economic and environmental analyses could be the object of future studies based on the results of this research work.

From the analysis of the exergy improvement potential, this study also suggests that efforts to improve the thermodynamic performance should focus on the gasification and drying units, due to their high exergy improvement potential. Regarding the gasification unit, it has been discussed that there is room for improvement in the cold gas efficiency, mainly when steam is used as a gasification medium mixed with air

The results obtained in this work revealed that the gasification of giant reed and its integration with power generation or cogeneration systems is valuable and deserves massive deployment in those regions where the feedstock is available. Indeed, the impacts of energy production from this feedstock can be relevant whether cultivated as an energy crop or obtained from land management activities. Hence, an important implication is that, thanks to the results of this research work, case studies of local or regional bioenergy systems based on giant reed as feedstock for the decarbonization of the electricity grid with a programmable and renewable energy source can be developed.

#### 4.2. Limitations and future research directions

A limitation of the present study for the comparative analysis of the two layouts is intentionally the absence of an economic analysis. The authors' goal is, indeed, to focus on the detailed thermodynamic analysis of the proposed layouts within the limitations of the manuscript length. It follows that the next research step will be the economic and thermoeconomic analysis of the proposed layouts, along with integrating such processes in a real context for case-study development, using the outcomes of the present study. Furthermore, considering the uncovered promising potentials of Arundo Donax gasification, broader operating conditions should be assessed on larger-scale reactors, aiming at validating the presented data and optimizing the gasification unit by improving the conversion efficiency and reducing the exergy loss. The same approach should involve the drying unit, as evidenced by the potential indicator of exergy improvement. The improvements of these units will potentially lead to a significant enhancement of the whole bioenergy process.

The detailed and comparative exergy analysis carried out in this research work, the related results, and the methods applied can be exploited by the scientific community for replicating the simulation model and developing case studies and tools for decision-making.

# CRediT authorship contribution statement

Mauro Prestipino: Writing – original draft, Visualization, Software, Methodology, Investigation, Formal analysis, Data curation, Conceptualization. Antonio Piccolo: Writing – review & editing, Supervision, Methodology, Formal analysis. Carlos Mourao Vilela: Writing – review & editing, Project administration, Investigation, Funding acquisition. Antonio Galvagno: Writing – review & editing, Supervision, Project administration, Funding acquisition, Conceptualization.

#### **Declaration of competing interest**

The authors declare the following financial interests/personal relationships which may be considered as potential competing interests: Mauro Prestipino reports financial support was provided by European Commission. If there are other authors, they declare that they have no known competing financial interests or personal relationships that could have appeared to influence the work reported in this paper.

#### References

[1] Y. Sun, Y. Li, R. Wang, R. Ma, Assessing the national synergy potential of onshore and offshore renewable energy from the perspective of resources dynamic and

- complementarity, Energy 279 (2023) 128106, https://doi.org/10.1016/j.
- [2] F. Cao, Digital financial innovation and renewable electrification: a step toward zero carbon nexus, Renew. Energy 215 (2023) 118910, https://doi.org/10.1016/j.
- [3] A. Nadolny, C. Cheng, B. Lu, A. Blakers, M. Stocks, Fully electrified land transport in 100% renewable electricity networks dominated by variable generation, Renew. Energy 182 (2022) 562-577, https://doi.org/10.1016/j.renene.2021.10.039.
- [4] F. Levihn, CHP and heat pumps to balance renewable power production: lessons from the district heating network in stockholm, Energy 137 (2017) 670-678, oi.org/10.1016/j
- [5] G. Squadrito, G. Maggio, A. Nicita, The green hydrogen revolution, Renew. Energy (2023) 119041, https://doi.org/10.1016/j.renene.2023.119041.
- [6] T. Nguyen, L. Gustavsson, Production of district heat, electricity and/or biomotor fuels in renewable-based energy systems, Energy 202 (2020) 117672, https://doi.
- [7] M. ElSayed, A. Aghahosseini, C. Breyer, High cost of slow energy transitions for emerging countries: on the case of Egypt's pathway options, Renew. Energy 210 (2023) 107-126, https://doi.org/10.1016/j.renene.2023.04.03
- [8] G.S. Seck, V. Krakowski, E. Assoumou, N. Maïzi, V. Mazauric, Embedding power system's reliability within a long-term energy system optimization model: linking high renewable energy integration and future grid stability for France by 2050, Appl. Energy 257 (2020) 114037, https://doi.org/10.1016/j penergy, 2019, 114037.
- [9] H. Lund, I.R. Skov, J.Z. Thellufsen, P. Sorknæs, A.D. Korberg, M. Chang, B. V. Mathiesen, M.S. Kany, The role of sustainable bioenergy in a fully decarbonised society, Renew. Energy 196 (2022) 195-203, https://doi.org/10.1016/j renene.2022.06.026
- [10] M. Prestipino, A. Piccolo, M.F. Polito, A. Galvagno, Combined bio-hydrogen, heat, and power production based on residual biomass gasification: energy, exergy, and renewability assessment of an alternative process configuration, Energies 15 (2022), https://doi.org/10.3390/en15155524.
- [11] C. Blasio, De Fundamentals of Biofuels Engineering and Technology, 2019, p. 429. ISBN 9783030115982.
- K.J. Ptasinski, Efficiency of Biomass Energy: an Exergy Approach to Biofuels, [12] Power, and Biorefineries, 2016. ISBN 9781119118169.
- [13] M. Prestipino, F. Salmeri, F. Cucinotta, A. Galvagno, Thermodynamic and environmental sustainability analysis of electricity production from an integrated cogeneration system based on residual biomass: a life cycle approach, Appl. Energy 295 (2021), https://doi.org/10.1016/j.apenergy.2021.117054
- [14] K. Difs, E. Wetterlund, L. Trygg, M. Söderström, Biomass gasification opportunities in a district heating system, Biomass Bioenergy 34 (2010) 637-651, https://doi. g/10.1016/i.biombioe.2010.01.007.
- [15] M. Soffiato, C.A. Frangopoulos, G. Manente, S. Rech, A. Lazzaretto, Design optimization of ORC systems for waste heat recovery on board a LNG carrier, Energy Convers. Manag. 92 (2015) 523-534, https://doi.org/10.1016/j. enconman, 2014, 12, 085.
- [16] B.R. Bakshi, T.G. Gutowski, D.P. Sekulic, Thermodynamics and the Destruction of
- Resources, Cambridge University Press, New York, 2011. ISBN 978-1-107-68414-0.

  [17] T.J. Kotas, The Exergy Method of Thermal Plant Analysis, Exergon Publishing Company, London, 2012. ISBN 978-1-908341-89-1.
- [18] H.Æ. Sigurjonsson, L.R. Clausen, Solution for the future smart energy system: a polygeneration plant based on reversible solid oxide cells and biomass gasification producing either electrofuel or power, Appl. Energy 216 (2018) 323-337, https:// oi.org/10.1016/j.apenergy.2018.02.124.
- [19] J. François, G. Mauviel, M. Feidt, C. Rogaume, Y. Rogaume, O. Mirgaux, F. Patisson, A. Dufour, Modeling of a biomass gasification CHP plant: influence of various parameters on energetic and exergetic efficiencies, Energy Fuel. 27 (2013) 7398-7412, https://doi.org/10.1021/ef4011466.
- [20] Z. Wu, P. Zhu, J. Yao, S. Zhang, J. Ren, F. Yang, Z. Zhang, Combined biomass gasification, SOFC, IC engine, and waste heat recovery system for power and heat generation: energy, exergy, exergoeconomic, environmental (4E) evaluations, Appl. Energy 279 (2020) 115794, https://doi.org/10.1016/j. ergv.2020.115794
- [21] N. Kabalina, M. Costa, W. Yang, A. Martin, M. Santarelli, Exergy analysis of a polygeneration-enabled district heating and cooling system based on gasification of refuse derived fuel, J. Clean. Prod. 141 (2017) 760-773, https://doi.org/10.1016/
- [22] F. Yang, H. Zhang, Z. Yu, E. Wang, F. Meng, H. Liu, J. Wang, Parametric optimization and heat transfer analysis of a dual loop ORC (organic rankine cycle) system for CNG engine waste heat recovery, Energy 118 (2017) 753-775, https:// oi.org/10.1016/j.energy.2016.10.119.
- [23] V. Badescu, M.H.K. Aboaltabooq, H. Pop, V. Apostol, M. Prisecaru, T. Prisecaru, Design and operational procedures for ORC-based systems coupled with internal combustion engines driving electrical generators at full and partial load, Energy Convers. Manag. 139 (2017) 206-221, https://doi.org/10.1016/ nconman 2017 02 046
- [24] S. Khanmohammadi, K.Energy Atashkari, Exergy, and environmental analyses of a poly-generation system based on biomass gasification, Fuel 320 (2022) 123963, /doi.org/10.1016/j.fuel.2022.1239
- [25] A. Behzadi, E. Gholamian, E. Houshfar, A. Habibollahzade, Multi-objective optimization and exergoeconomic analysis of waste heat recovery from tehran's waste-to-energy plant integrated with an ORC unit, Energy 160 (2018) 1055-1068, energy.2018.07.074.
- [26] N. Manić, B. Janković, D. Stojiljković, M. Popović, S. Cvetković, H. Mikulčić, Thermodynamic study on energy crops thermochemical conversion to increase the

- efficiency of energy production, Thermochim. Acta 719 (2023), https://doi.org/
- E. Pienihäkkinen, E.J. Leijenhorst, W. Wolters, C. Lindfors, J. Lahtinen, T. Ohra-Aho, A. Oasmaa, Valorization of Eucalyptus, giant reed Arundo, fiber sorghum, and sugarcane bagasse via fast pyrolysis and subsequent bio-oil gasification, Energy Fuel. 36 (2022) 12021-12030, https://doi.org/10.1021/acs.energyfuels.2c01968.
- [28] C. Dupont, R. Chiriac, G. Gauthier, F. Toche, Heat capacity measurements of various biomass types and pyrolysis residues, Fuel 115 (2014) 644-651, https:// doi.org/10.1016/j.fuel.2013.07.086.
- [29] A. Galvagno, M. Prestipino, S. Maisano, F. Urbani, V. Chiodo, Integration into a citrus juice factory of air-steam gasification and CHP system: energy sustainability assessment, Energy Convers. Manag. (2019) 74-85, https://doi.org/10.1016/j.
- [30] H. Visser, R. Zwart, J. Konemann, A. Bos, J. Kuipers, Rdf-Gasification Part 1: Characterizing the Use of Rdf as Fuel and Solving the Tar Problem by an In-Depth Laboratory Study, 2009.
- [31] N. Cerone, F. Zimbardi, L. Contuzzi, E. Alvino, M.O. Carnevale, V. Valerio, Updraft gasification at pilot scale of hydrolytic lignin residue, Energy Fuel. 28 (2014) 3948-3956, https://doi.org/10.1021/ef
- [32] S. You, H. Tong, J. Armin-Hoiland, Y.W. Tong, C.H. Wang, Techno-economic and greenhouse gas savings assessment of decentralized biomass gasification for electrifying the rural areas of Indonesia, Appl. Energy 208 (2017) 495-510, https://doi.org/10.1016/j.apenergy.2017.10.001
- [33] M. Soffiato, C.A. Frangopoulos, G. Manente, A. Lazzaretto, Design and performance evaluation of an organic rankine cycle system exploiting the low grade waste heat of the main engines in a LNG carrier. Proceedings of the 27th International Conference on Efficiency, Cost, Optimization, Simulation and Environmental Impact of Energy Systems, ECOS 2014, 2014.
- [34] D.S. Østergaard, S. Svendsen, Costs and benefits of preparing existing Danish buildings for low-temperature district heating, Energy 176 (2019) 718-727, 10.1016/j.energy.2019.03.186
- [35] A.A. Sinha, G. Saini, Sanjay, A.K. Shukla, M.Z. Ansari, G. Dwivedi, T. Choudhary, A novel comparison of energy-exergy, and sustainability analysis for biomassfueled solid oxide fuel cell integrated gas turbine hybrid configuration, Energy Convers. Manag. 283 (2023) 116923, https://doi.org/10.1016/j enconman.2023.116923.
- [36] A. Midilli, I. Dincer, Development of some exergetic parameters for PEM fuel cells for measuring environmental impact and sustainability, Int. J. Hydrogen Energy 34 (2009) 3858–3872, https://doi.org/10.1016/j.ijhydene.2009.02.066.
- [37] M. Prestipino, A. Galvagno, O. Karlström, A. Brink, Energy conversion of agricultural biomass char: steam gasification kinetics, Energy 161 (2018), https:// doi.org/10.1016/i.energy.2018.07.205
- N.D. Couto, V.B. Silva, E. Monteiro, A. Rouboa, P. Brito, An experimental and numerical study on the Miscanthus gasification by using a pilot scale gasifier, Renew. Energy 109 (2017) 248-261, https://doi.org/10.1016/j. renene, 2017, 03, 028,
- [39] X. Ge, F. Xu, J. Vasco-Correa, Y. Li, Giant reed: a competitive energy crop in comparison with Miscanthus, Renew. Sustain. Energy Rev. 54 (2016) 350-362, https://doi.org/10.1016/j.rser.2015.10.010.
- [40] T.L.T. Nguyen, J.E. Hermansen, Life cycle environmental performance of Miscanthus gasification versus other technologies for electricity production, Sustain, Energy Technol, Assessments 9 (2015) 81-94, https://doi.org/10.1016/j. eta 2014 12 00
- [41] T. Soleimani, F. Sordes, I. Techer, G. Junqua, M. Hayek, M. Salgues, J.C. Souche, Comparative environmental and economic life cycle assessment of phytoremediation of dredged sediment using Arundo Donax, integrated with biomass to bioenergy valorization chain, Sci. Total Environ. 903 (2023), https:// doi org/10 1016/i scitoteny 2023 166160.
- [42] G. Allesina, S. Pedrazzi, F. Ginaldi, G.A. Cappelli, M. Puglia, N. Morselli, P. Tartarini, Energy production and carbon sequestration in wet areas of emilia romagna region, the role of Arundo Donax, Adv. Model. Anal. 55 (2018) 108-113, ttps://doi.org/10.18280/ama a.550302
- [43] E. Ceotto, C. Vasmara, R. Marchetti, S. Cianchetta, S. Galletti, Biomass and methane yield of giant reed (Arundo Donax L.) as affected by single and double annual harvest, GCB Bioenergy 13 (2021) 393-407, https://doi.org/10.1111/ cbb 12790
- [44] E. Alexopoulou, F. Zanetti, D. Scordia, W. Zegada-Lizarazu, M. Christou, G. Testa, S.L. Cosentino, A. Monti, Long-term yields of switchgrass, giant reed, and Miscanthus in the mediterranean basin, Bioenergy Res 8 (2015) 1492-1499, https://doi.org/10.1007/s12155-015-9687-x
- [45] S.A. Corinzia, B.R. Ciaramella, A. Piccitto, G. Testa, C. Patanè, S.L. Cosentino, D. Scordia, The response of lignocellulosic perennial grasses to different soil water availability, European Biomass Conference and Exhibition Proceedings (2021) 345-351
- [46] M.J. Prins, K.J. Ptasinski, F.J.J.G. Janssen, Thermodynamics of gas-char reactions: first and second law analysis, Chem. Eng. Sci. 58 (2003) 1003-1011, https://doi rg/10.1016/S0009-2509(02)00641-3
- [47] W. Sun, X. Yue, Y. Wang, Exergy efficiency analysis of ORC (organic rankine cycle) and ORC-based combined cycles driven by low-temperature waste heat, Energy

- Convers. Manag. 135 (2017) 63–73, https://doi.org/10.1016/j.enconman.2016.12.042.
- [48] G. Davies, H. Lagoeiro, H. Turnell, M. Wegner, A. Foster, J. Evans, A. Revesz, A. Leiper, K. Smyth, J. Hamilton, et al., Evaluation of low temperature waste heat
- [49] E. Monteiro, A. Ramos, A. Rouboa, Fundamental designs of gasification plants for combined heat and power, Renew. Sustain. Energy Rev. 196 (2024) 114305, https://doi.org/10.1016/j.rser.2024.114305.